Supplementary Information:

Snapshot macroscopic Fourier ptychography: far-field synthetic aperture imaging via illumination multiplexing and camera-array acquisition

Sheng Li[1,2], Bowen Wang[1,2], Haitao Guan[1,2], Qian Chen[1,2,*], and Chao Zuo[1,2,]**

[1]School of Electronic and Optical Engineering, Nanjing University of Science and Technology, No. 200 Xiaolingwei Street, Nanjing, Jiangsu Province 210094, China.
[2]Smart Computational Imaging Laboratory (SCILab), Nanjing University of Science and Technology, Nanjing, Jiangsu Province 210094, China.
[3]Jiangsu Key Laboratory of Spectral Imaging & Intelligent Sense, Nanjing, Jiangsu Province 210094, China.
[*]chenqian@njust.edu.cn
[**]zuochao@njust.edu.cn

ABSTRACT

This document provides supplementary information to “Snapshot macroscopic Fourier ptychography: far-field synthetic aperture imaging via illumination multiplexing and camera-array acquisition”.

Contents:

A. Analysis of the influence of sub-aperture distribution on reconstruction in Fourier ptychographic microscopy and macroscopic Fourier ptychography

The Illumination-Multiplexed Snapshot Synthetic Aperture Imaging (IMSS-SAI) technique integrates illumination multiplexing with a camera array to facilitate single-shot synthetic aperture imaging. In a camera array imaging system, even adjacent cameras cannot merge with each other, so there is no overlapping ratio between the sub-apertures. Therefore, multiplexing illumination in IMSS-SAI is employed to ensure the necessary overlap between sub-apertures. In contrast, in Fourier ptychographic microscopy (FPM), the synthetic aperture is achieved by illuminating the sample from different incident angles by using an LED array. As the units in an LED array are arranged more closely, the overlapping ratio between the sub-apertures increases accordingly. Generally, in FPM, the overlapping ratio between sub-apertures needs to exceed 39.1%; otherwise, the iterative reconstruction may fail to converge correctly. Figure S1(a1) gives a typical example of an aperture arrangement with a low-overlapping ratio, in which case it is quite difficult for FPM to obtain a correct synthetic aperture result(shown in Fig. S1(a2)) without additional intensity measurements or regularization algorithm. The sub-cameras in IMSS-SAI are equally spaced and non-overlapping ratio, and their outer boundary forms a square shape, as shown in Fig. S1(b1). The main difference between IMSS-SAI and traditional FPM is whether it can provide a sufficient overlapping ratio for the reconstruction process despite the physical limitation of no overlap between adjacent cameras.

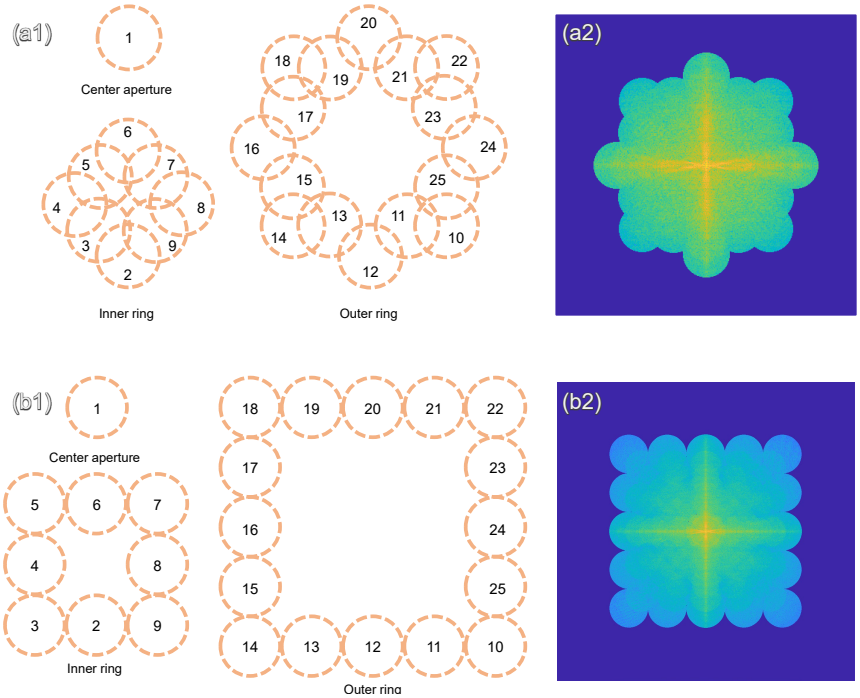

Fig. S1 Analysis of the influence of sub-aperture distribution. (a1) The distribution of sub aperture in FPM with low overlapping ratio. (a2) The corresponding spectrum of FPM. (b1) The distribution of sub aperture in camera array without overlapping ratio. (b2) The corresponding spectrum of the camera array.

Following the decoupling of the three-wavelength apertures, as per the illumination multiplexing method, the final layout of 75 sub-aperture images can be achieved from the raw images captured by the 5×5 camera array[1]. To accurately quantify the overlapping ratio between each sub-aperture, the spectrum shift components corresponding to the different wavelengths must be calculated. The aperture distribution, progressing from the center outward, includes the central aperture, the R/G/B channels in the inner ring, and the R/G/B channels in the outer ring. Additionally, the spectrum shift components differ across wavelengths, leading to varying overlapping ratios. To accurately calculate these ratios, we account for the differing cutoff frequencies (f_c) of adjacent channels. The calculation of the overlapping ratio can be expressed as: $overlap = S/\pi f_c^2$,while the S is the overlapping area can be written as:

$$S = 2\left[\pi f_c^2 \cdot \frac{2\theta}{2\pi} - \frac{1}{2} \cdot \frac{f_s}{2} \cdot 2\sqrt{f_c^2 - (f_s^2/2)^2}\right] \tag{S1}$$

where $\theta = \arccos \frac{f_s}{2f_c}$, since the cut-off frequencies of the R and B channels are different during calculating, we compute the overlapping ratio for the R channel in the inner ring based on the proportion of the overlapping area to the R channel. The calculated overlapping ratio for the R/G/B channels of apertures at different positions are shown in Table S1.

As indicated, the overlapping ratio between the inner ring and the central aperture remains above 50%, primarily because the sub-apertures of the R channel in the inner ring overlap with the B channel of the central aperture. The overlapping ratio between channels in the outer ring, excluding the diagonal, is above 80%, and even the overlapping ratio between channels on the diagonal is more than 60%. The decoupling images meet the redundancy requirements for successful reconstruction using FP. Attentively, if a single camera were used by changing its recording position(aperture scanning Fourier ptychography) instead of the IMSS-SAI method, it would require 121 scanning times to achieve the same four-fold resolution enhancement.

Table S1. Overlapping ratio of sub-aperture in camera array with R/G/B channels.

sub-apertures / Channels	[2.4.6.8]	[3,5,7,9]	[10,12,14,16,18,20,22,24]	[11,15,19,23]	[13,17,21,25]
R channel	63.79%	52.58%	73.49%	71.56%	66.43%
G channel	88.49%	83.73%	67.88%	60.24%	59.39%
B channel	82.66%	75.48%	79.34%	74.43%	73.87%

In practical experiments, the calculation of the overlapping ratio distribution for IMSS-SAI is complex. The limitation makes it difficult to compare the reconstructed results of IMSS-SAI with aperture-scanning Fourier ptychography under different overlapping ratios. As an alternative, we compared the reconstructed results under low and no overlap conditions in simulation experiments to demonstrate the robustness of IMSS-SAI. The simulations were performed based on the distributions shown in Fig. S1, and as reflected in the simulation results of the USAF resolution target in Fig. 3 of the main text.

To further supplement the simulation results in Fig. 3, we compared the reconstructed results of IMSS-SAI and aperture-scanning FP under both low-overlapping and no-overlapping conditions. Figure. S2(a1)

presents the synthetic aperture result using IMSS-SAI (without overlapping ratio, aperture distribution as shown in Fig. S1(b)) and Fig. S2(a2) is an enlarged area of the boxed portion of Fig. S2(a1), while Fig. S2(b1) shows the result under low-overlapping-ratio conditions (aperture distribution as shown in Fig. S1(a)) and Fig. S2(b2) is an enlarged area of the boxed portion of Fig. S2(b1). It can be observed that with a partial overlapping ratio, the imaging quality and resolution with the IMSS-SAI method remain consistent. The artifacts of the results in different overlapping ratios are slightly different. In contrast, Fig. S2(c1) shows the synthetic aperture results using aperture-scanning FP (without overlapping ratio, Fig. S2(c2) is an enlarged area of the boxed portion of Fig. S2(c1)), and Fig. S2(d) shows the result under low-overlapping-ratio conditions (Figure. S2(d2) is the enlarged area of the boxed portion of Fig. S2(d1)). The reconstructed results reveal some high-frequency information, but incorrect convergence has led to more severe artifacts. As the aperture-scanning FP results (Figure. S2(c1), and corresponding enlarged area Fig. S2(c2)) demonstrate, the line pairs in group -1 are incorrectly reconstructed. Even with a low-overlapping distribution, the reconstructed result fails to improve the image quality. Figure S2 demonstrates the robustness of IMSS-SAI, highlighting that it performs well even under challenging conditions characterized by a low overlap ratio.

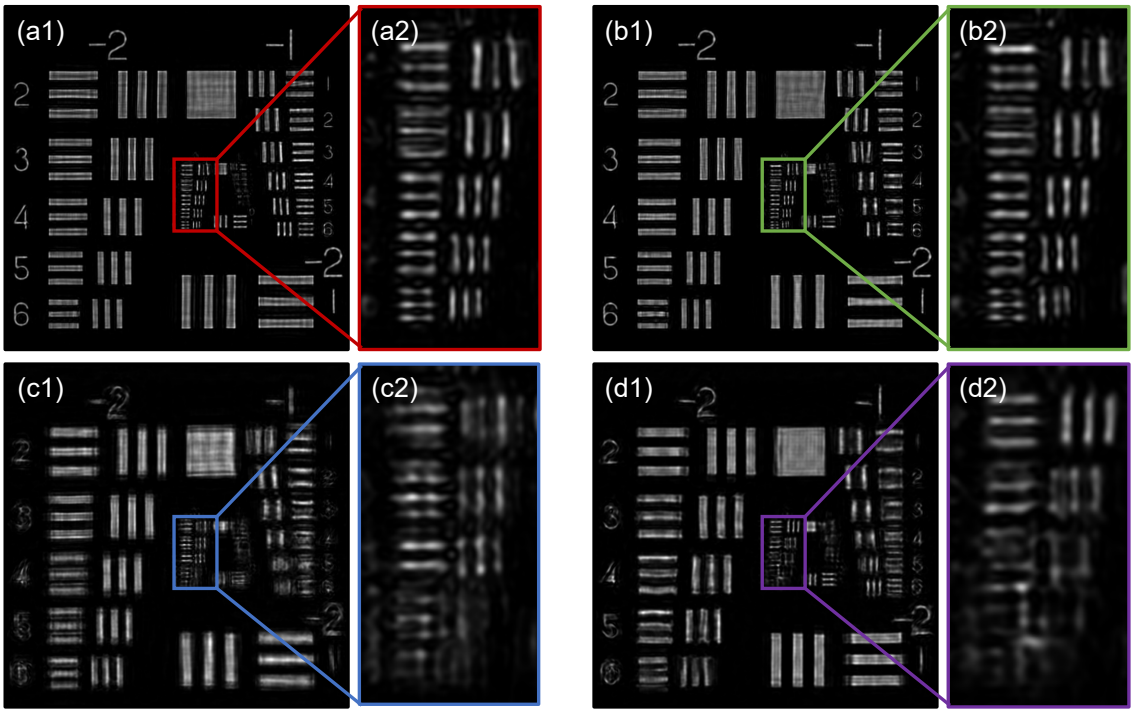

Fig. S2 Results of IMSS-SAI and aperture scanning FP with non-overlapping-ratio and low-overlapping-ratio conditions. (a1) The reconstructed result of IMSS-SAI with non-overlapping-ratio conditions. (a2) The enlarged area of the boxed portion of a1. (b1) The reconstructed result of IMSS-SAI with low-overlapping-ratio conditions. (b2) The enlarged area of the boxed portion of b1. (c1) The reconstructed result of aperture scanning FP with non-overlapping-ratio conditions. (c2) The enlarged area of the boxed portion of c1. (d1) The reconstructed result of aperture scanning FP with low-overlapping-ratio conditions. (d2) The enlarged area of the boxed portion of d1.

B. Analysis of aperture-scanning FP and IMSS-SAI reconstruction results using a Siemens star target

Macroscopic FP with a single camera typically requires hours of scanning, whereas IMSS-SAI enhances resolution with a single exposure. We simulated and compared the reconstruction results of the Siemens star using single-aperture scanning and IMSS-SAI. In the previous section, we presented the imaging results of the USAF resolution target. In this section, we utilize the Siemens star pattern to further validate the differences between the aperture scanning FP and IMSS-SAI methods. The Siemens star is advantageous because it continuously represents different spatial frequencies in various directions, making it an excellent sample for evaluating and demonstrating resolution performance. We use 121 low-resolution Siemens star images for aperture scanning and 25 low-resolution Siemens star images for IMSS-SAI. The F-number of the sub apertures was uniformly set to 22. Low-resolution images used for aperture scanning were based on the cutoff frequency of the B channel (images for IMSS-SAI contain the R/G/B channels). The sub-aperture image with blue light illumination is shown in Fig. S3(a), and the corresponding enlarged area of the boxed portion is shown in Fig. S3(a1). The reconstructed result using IMSS-SAI is shown in Fig. S3(b), and the corresponding enlarged area of the boxed portion is shown in Fig. S3(b1). The results from single-aperture scanning reconstruction (Figure S3(c) and the corresponding enlarged boxed area (c1)) and those from the IMSS-SAI method both achieved resolution enhancement through proper convergence. However, while the single-aperture scanning required approximately one hour to collect 121 images, the IMSS-SAI method only needed single exposure with 25 images.

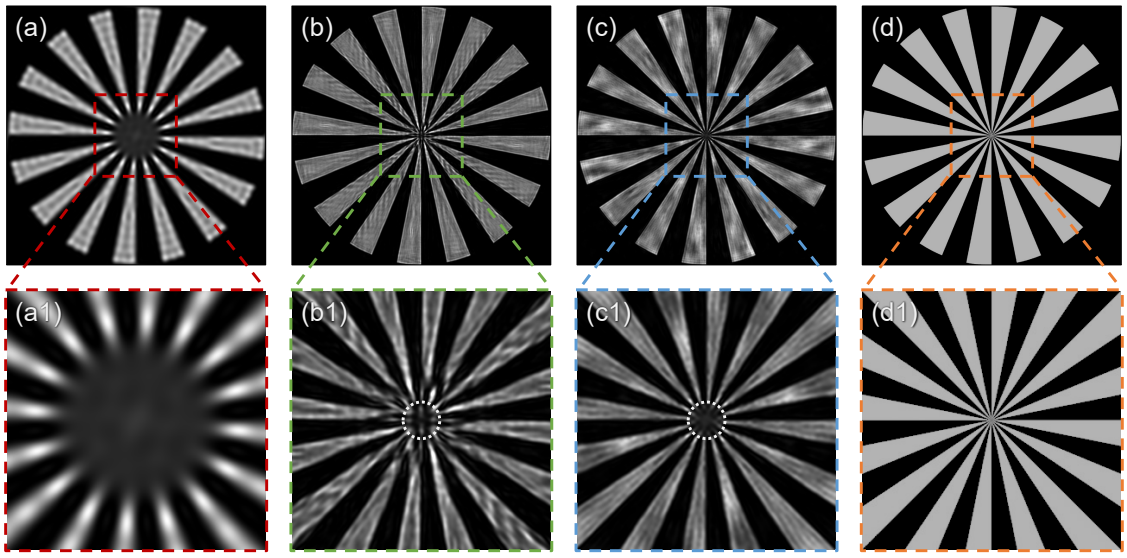

Fig. S3 Results of the Siemens star. (a) The sub-aperture image with blue light illumination and corresponding enlarged area of the boxed portion a1. (b) The reconstructed result using IMSS-SAI and corresponding enlarged area of the boxed portion b1. (c) The reconstructed result from single-aperture scanning (blue channel illumination) and corresponding enlarged area of the boxed portion c1. (d) The ground truth image of siemens star and corresponding enlarged area of the boxed portion d1.

C. Comparison of IMSS-SAI and single-channel independent reconstruction for imaging smooth target

While the synthesized spectrum regions of IMSS-SAI and single-channel FP remain consistent, the critical distinction lies in the insufficient redundancy of the single-channel approach. This limitation impedes the accurate recovery of the target's complex amplitude during the iterative reconstruction process. Using color camera to record images in FPM can directly separate channels, thus bypassing the decoupling process. Unlike in the past, IMSS-SAI uses a monochrome camera for iterative decoupling of the three illumination channels, enhancing photon efficiency and preventing color leakage and crosstalk. For distant objects, a high-resolution reconstruction image can be attained by approximating the intensity responses of the R/G/B channels as uniform. Despite the phase responses across the three channels may be inconsistent resulting in artifacts[2], these artifacts have minimal effect on the reconstructed intensity image. Additionally, we mitigate the impact of the artifacts by incorporating total variation regularization constraints into the reconstruction process. We conducted simulation comparisons between the reconstruction results of IMSS-SAI and single-channel reconstruction, particularly focusing on the results of individual reconstruction of the three channels, as shown in Fig. S4.

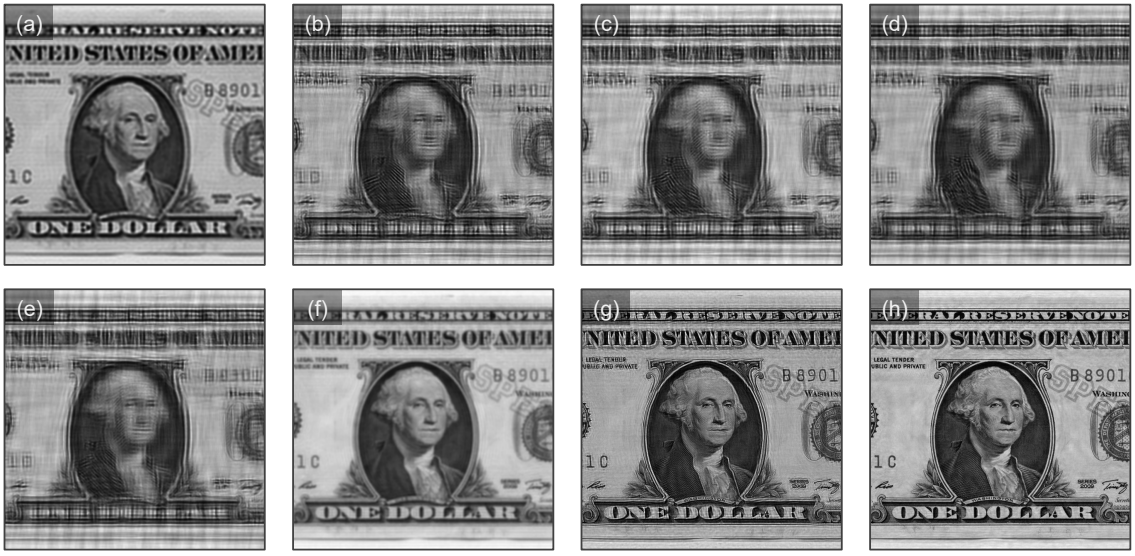

Fig. S4 The comparison of IMSS-SAI and single-channel independent reconstruction for imaging smooth target. (a) The sub-aperture image with blue light illumination. (b) The reconstructed result of the single R channel by aperture scanning. (c) The reconstructed result of the single G channel by aperture scanning. (d) The reconstructed result of the single B channel by aperture scanning. (e) The result after independently reconstructing each channel using aperture scanning and then averaging these reconstructions. (f) The result of directly averaging the sub-aperture images from all three channels without performing independent reconstructions. (g) The reconstructed result with IMSS-SAI. (h) The reconstructed result of B channel with high overlapping ratio (76%).

The superimposed images of the three channels under a single aperture are depicted in Fig. S4(a), while Fig. S4(b) displays reconstructed result of single R channel by aperture scanning. Figure. S4(c) displays reconstructed result of single G channel by aperture scanning and Fig. S4(d) displays reconstructed result of single G channel. Figure. S4(e) shows the reconstructed result obtained by independently reconstructing each channel using aperture scanning and then averaging these results. As illustrated, the single-channel reconstruction introduces significant errors because we cannot accurately retrieve the phase information. Averaging the reconstructed results from three channels, can only marginally improve image quality and fails to mitigate artifacts. Figure. S4(f) represents the averaging result of the 25 sub-aperture images directly. Figure. S4(g) displays the reconstructed result of IMSS-SAI, while Fig. S4(h) shows the reconstructed result with a high overlapping ratio in the blue channel. Consistent with the results in Fig. S3, the IMSS-SAI reconstructed result closely matches that of the high-overlapping ratio (76%) reconstructed result, both achieving a four-fold resolution enhancement.

D. Comparison of IMSS-SAI and single-channel independent reconstruction for imaging rough target

The prerequisite for achieving high-resolution reconstruction with IMSS-SAI is to approximate image intensity recorded at three wavelengths as the same intensity, i.e., the intensity responses of samples are nearly the same across different spectrum channels. In Section C, we verified that the reconstruction results for smooth targets meet the intensity response approximation. For rough targets, the diffuse reflection process uniformly mixes high-frequency and low-frequency information into the spectrum. The spectrum distribution across three channels does not exhibit significant differences in response to intensity information, thus the approximation conditions for IMSS-SAI are still satisfied. To validate the accuracy of the approximation calculation, we reconstructed the captured target image and compared the results of IMSS-SAI with those of single-wavelength under low redundancy conditions. Although the speckle noise contained in the raw sub-aperture intensity measurements can be suppressed by taking the averaging method[3], the resolution of the target cannot be further improved. To balance the enhancement of resolution, we utilize the data redundancy in the raw measurements and the total variation regularization employed in our reconstruction algorithm, which significantly mitigates the speckle noise.

Figures. S5(a, b, c) respectively represent the results of sub-aperture image reconstruction of the R/G/B channels decoupled using the state-multiplexed Fourier ptychography algorithm. It can be observed that under low redundancy conditions, the reconstructed results of all three channels fail to get convergence because lacking the correct phase information. Figure. S5(d) shows the reconstructed result obtained by independently reconstructing each channel using aperture scanning and then averaging these results. Compared to the reconstructed results of individual wavelengths, the averaging method only suppresses speckle noise, but fails to improve the resolution. Figure. S5(e) displays the result of directly averaging the sub-aperture images from all three channels. Different with Fig. S5(d), the process of averaging in Fig. S5(e) does not require the reconstruction. Figure. S5(f) shows the reconstructed result of IMSS-SAI.The high signal-to-noise ratio and high-resolution reconstructions obtained by the IMSS-SAI method

demonstrate that by iteratively reconstructing the sub-aperture images of the R/G/B channels on the same image, IMSS-SAI significantly suppresses the influence of speckle noise while enhancing image resolution.

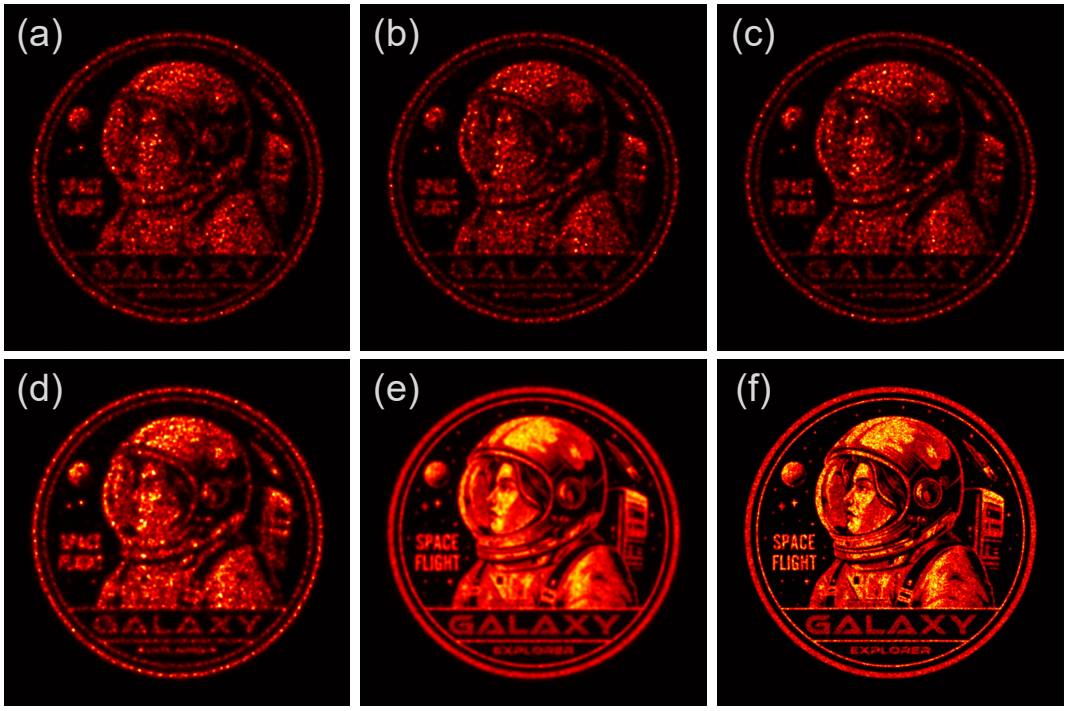

Fig. S5 Experimental results of astronaut stickers. (a) The reconstructed result of single R channel by aperture scanning. (b) The reconstructed result of single G channel by aperture scanning. (c) The reconstructed result of single B channel by aperture scanning. (d) The result after independently reconstructing each channel using aperture scanning and then averaging these reconstructions. (e) The result of directly averaging the sub-aperture images from all three channels without performing independent reconstructions. (f) The reconstructed result of IMSS-SAI.

.

References

1. Dong, S., Shiradkar, R., Nanda, P. & Zheng, G. Spectral multiplexing and coherent-state decomposition in Fourier ptychographic imaging. *Biomedical Optics Express* **5**, 1757 (2014). URL https://opg.optica.org/boe/abstract.cfm?uri=boe-5-6-1757. DOI 10.1364/BOE.5.001757.

2. Dong, S. *et al.* Aperture-scanning Fourier ptychography for 3D refocusing and super-resolution macroscopic imaging. *Optics Express* **22**, 13586–13599 (2014). URL https://opg.optica.org/oe/abstract.cfm?uri=oe-22-11-13586. DOI 10.1364/OE.22.013586. Publisher: Optica Publishing Group.

3. Holloway, J., Wu, Y., Sharma, M. K., Cossairt, O. & Veeraraghavan, A. SAVI: Synthetic apertures for long-range, subdiffraction-limited visible imaging using Fourier ptychography. *Science advances* **3**, e1602564 (2017).